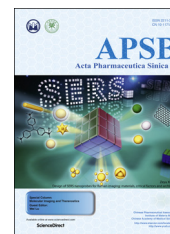




Chinese Pharmaceutical Association  
Institute of Materia Medica, Chinese Academy of Medical Sciences

Acta Pharmaceutica Sinica B

[www.elsevier.com/locate/apsb](http://www.elsevier.com/locate/apsb)  
[www.sciencedirect.com](http://www.sciencedirect.com)



REVIEW

# Surface-enhanced Raman nanoparticles for tumor theranostics applications



Yangyang Li<sup>a,b</sup>, Qiaolin Wei<sup>a,b</sup>, Fei Ma<sup>a,b</sup>, Xin Li<sup>c</sup>, Fengyong Liu<sup>c,\*</sup>,  
Min Zhou<sup>a,b,d,\*\*</sup>

<sup>a</sup>Department of Nuclear Medicine & Key Laboratory of Cancer Prevention and Intervention, National Ministry of Education, The Second Affiliated Hospital, School of Medicine, Zhejiang University, Hangzhou 310009, China

<sup>b</sup>Institute of Translational Medicine, Zhejiang University, Hangzhou 310009, China

<sup>c</sup>Department of Interventional Radiology, Chinese PLA General Hospital, Beijing 100853, China

<sup>d</sup>State Key Laboratory of Modern Optical Instrumentations, Zhejiang University, Hangzhou 310058, China

Received 14 January 2018; received in revised form 7 March 2018; accepted 14 March 2018

## KEY WORDS

Raman spectroscopy;  
SERS;  
Cancer imaging;  
Nanoparticles;  
Theranostics

**Abstract** Raman spectroscopy, amplified by surface-enhanced Raman scattering (SERS) nanoparticles, can provide an *in vivo* imaging modality due to its high molecular specificity, high sensitivity, and negligible autofluorescence. The basis, composition, and methodologies developed for SERS nanoparticles are herein described. The research hotspots that are the focus in this paper are tumor imaging-guided theranostics and biosensing. The next breakthrough may be the development of biocompatible SERS nanoparticles and spectroscopic devices for clinical applications.

© 2018 Chinese Pharmaceutical Association and Institute of Materia Medica, Chinese Academy of Medical Sciences. Production and hosting by Elsevier B.V. This is an open access article under the CC BY-NC-ND license (<http://creativecommons.org/licenses/by-nc-nd/4.0/>).

\*Corresponding author.

\*\*Corresponding author at: Department of Nuclear Medicine & Key Laboratory of Cancer Prevention and Intervention, National Ministry of Education, The Second Affiliated Hospital, School of Medicine, Zhejiang University, Hangzhou 310009, China.

E-mail addresses: [fengyongliu@aliyun.com](mailto:fengyongliu@aliyun.com) (Fengyong Liu); [zhoum@zju.edu.cn](mailto:zhoum@zju.edu.cn) (Min Zhou).

Peer review under responsibility of Institute of Materia Medica, Chinese Academy of Medical Sciences and Chinese Pharmaceutical Association.

## 1. Background on the Raman effect

When light contacts matter, the majority of photons are scattered elastically by the Rayleigh effect<sup>1</sup>. However, a small minority of photons undergo a different scattering mechanism (inelastic scattering), where an energy exchange occurs during the interaction between the incident photon and the scattering material<sup>2</sup>. Raman spectroscopy is a vibrational spectroscopy technique that is based on the inelastic scattering of light by the targeted materials and provides a fingerprint of characteristic features<sup>3</sup>. The phenomenon of the Raman effect was first discovered experimentally by an Indian physicist named C.V.Raman in 1928<sup>4</sup>, who was awarded the Noble Prize in 1930. However, the sensitivity of Raman spectroscopy is intrinsically low. Moreover, Raman spectroscopy was not utilized for tracing analysis and surface science due to the nominal number of probe molecules<sup>5</sup>.

In 1974 Fleischmann et al.<sup>6</sup> experimentally observed clear, enhanced Raman signals from pyridine molecules attached to a roughened silver electrode. However, they attributed the increased Raman signals to the increase in adsorbed pyridine molecules due to the enlarged surface area of the corrugated surface. In 1977 enhanced Raman signals had been carefully calculated by Van Duyne et al.<sup>7</sup> and they concluded that the anomalously intense Raman signal should be attributed to enhanced Raman scattering efficiency, which was known as surface-enhanced Raman scattering (SERS)<sup>8</sup>.

The discovery of the SERS phenomenon greatly stimulated interest in surface-enhanced Raman studies<sup>9,10</sup>. As a result, the previously low tracking sensitivity has been improved enormously in surface Raman spectroscopy. Signals from the molecules adsorbed on metal nanostructures can be increased greatly, while the isolated molecules remain unchanged<sup>11,12</sup>. Furthermore, SERS can be used to reflect basic information on the targeted molecules with regard to surface orientation, bonding, and confirmation of the adsorbed molecules on the surface<sup>13</sup>. Interface reactions/biological processes also can be detected by SERS<sup>14,15</sup>. Therefore, SERS is an excellent technique for the characterization of molecules and amplification of molecular signals from molecules bound to or near plasmonic surfaces<sup>16</sup>. As for the mechanism of surface enhancement, it remains controversial. Generally, there are two accepted physical models, namely the surface-enhanced physical model and the surface-enhanced chemical model<sup>17,18</sup>.

## 2. SERS nanoparticles

Research on SERS is mainly focused on the fabrication of substrates, which are now divided into two major categories: tip-enhanced Raman spectroscopy (TERS)<sup>19–21</sup> and the preparation of nanoparticle substrate<sup>22–24</sup>. When metal materials are shaped into very small tip morphology, the molecules adsorbed induced an enhanced Raman spectroscopy called TERS. However, the development of TERS is only in the early stages. Another research direction is nanoparticle morphology. The shape and surface feature of the nanoparticles are important factors affecting the SERS performance<sup>25–29</sup>. Meanwhile, the distance between the nanoparticle substrates and the measured molecules plays a vital role in promoting the Raman signal from the targeted molecules. Moreover, the diverse morphology of nanoparticles may increase the possibility of a particular distance being suitable for SERS<sup>30,31</sup>. Currently, the basic shape of SERS nanoparticles includes spherical, rod, star and prismatic, as well as others<sup>32,33</sup>. The research direction of SERS is no longer limited to search for appropriate substrates; instead, the development of SERS

nanoparticles for medical applications has become the current mainstream direction<sup>34–36</sup>.

For biomedical applications, integrating the SERS amplification theory into nanoparticles with the properties of *in vitro* sensing, and further to develop these nanoparticles for *in vivo* imaging was the logical approach<sup>37–39</sup>. However, several factors should be considered, and hurdles had to be overcome before the use of SERS nanoparticles *in vivo*. Firstly, the selected material must have high SERS enhancement. The three best known SERS materials are silver<sup>40</sup>, gold<sup>41</sup> and copper<sup>42</sup> and have the advantage of being the most inert materials and thus providing the best possibilities for clinical applications<sup>43–45</sup>. Previous studies on silver<sup>46</sup> (Fig. 1) and gold<sup>47,48</sup> (Fig. 2) nanocomplexes have yielded numerous uses in biomedical applications. Secondly, the components of SERS nanoparticles should have the sufficient biocompatibility, that is, during the process of nanoparticle synthesis, potentially toxic elements or surfactants should be avoided as possible<sup>49</sup>. Finally, SERS nanoparticles should be encapsulated to ensure that the Raman reporter is isolated from external stimuli when used *in vivo*, to preserve the unique identifying Raman fingerprint and maintain its detection performance<sup>50</sup>. For instance, gold nanoparticles are often encapsulated into a silica shell or polyethylene glycol (PEG) and bound to bovine serum albumin (BSA) for stability or to protect the SERS probes<sup>51</sup>.

Generally, the *in vivo* SERS imaging strategy consists of bonding the SERS nanoparticles with Raman molecule probes attached to the nanoparticulate surface. As discussed above, SERS-active cores should be protected by other shell materials. Some researchers have synthesized Au@Raman probe@SiO<sub>2</sub> nanoparticles for SERS applications<sup>52</sup>. Briefly, a certain size of Au colloid was synthesized, mixed with a Raman probe or added in the presence of a coupling agent and then coated with a thinner silica shell (Fig. 3)<sup>53</sup>. Polymers possess distinctive advantages such as biocompatibility, biodistribution, and modifiability.

A SERS tag usually consists of a metal SERS nanoparticle core and adsorbed Raman probe molecules on the metal surface (Fig. 4)<sup>32</sup>. Subsequently, a modified biocompatible layer encases the metal particle and the Raman probe molecules and the surface can be functionalized further with targeting agents. The core of SERS tags is commonly gold nanoparticles which are considered to be chemically stable and nontoxic. The gold nanoparticles are plasmonically active in the NIR region, which is strongly favored for biomedical applications due to the low autofluorescence from tissues. Raman probe molecules with large Raman cross sections are often the superior choice for preparing SERS tags. Selecting probe molecules with an absorption spectrum that overlaps with the laser line (or the adsorption of SERS nanoparticle core) can lead to enhanced surface resonance Raman scattering.

SERS-active cores can also be modified by polymer materials<sup>54</sup>. One of the most common molecules is polyethylene glycol (PEG). A basic experimental route is carried out as follows: first, Au nanoparticles are modified with Raman probes and then attached with thiol-functionalized PEG that will stabilize the Raman signals in a harsh *in vivo* environment. The PEG shell can create a site to enhance the nanoparticles and prevent nonspecific interactions. In addition to silica and polymer shells, many researchers are also interested in molecular shells. A molecular shell can be formed with DNA molecules to form a special configuration<sup>55</sup>, such as a dimer mode, forming a gap between or within nanoparticles, and by using dye-labeled DNA sequences, the target on the solution or the substrate can be detected directly. Besides DNA, amino acids, peptides, and other kinds of molecules can be used for molecular shells and have a wide range of applications.

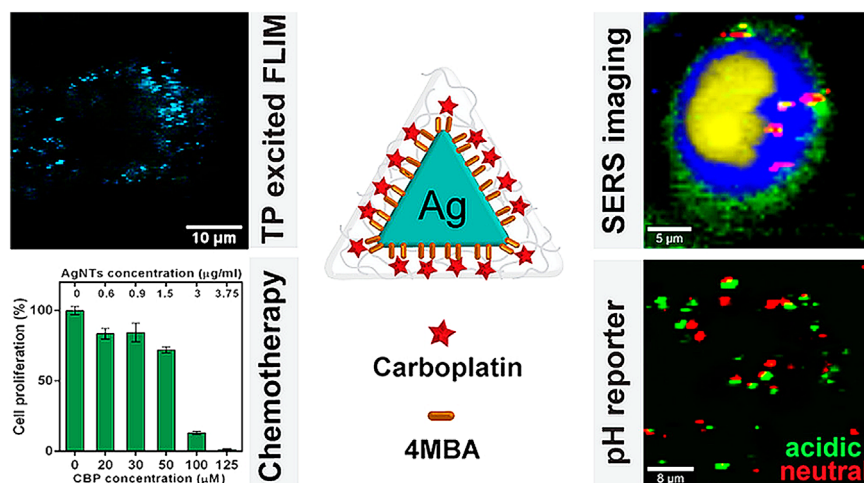


**Figure 1** Scheme of carboplatin-loaded, Raman-encoded, chitosan-coated silver nanotriangles as multimodal traceable nanotherapeutic delivery systems and pH reporters inside ovarian cancer cells. Reproduced with permission from ACS article<sup>46</sup>.

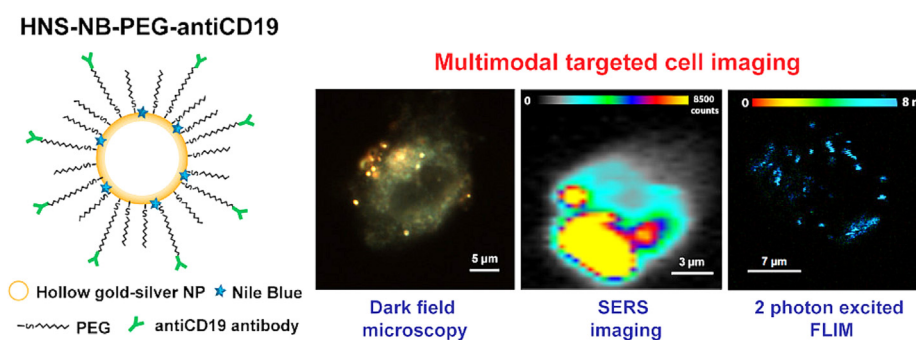


**Figure 2** Scheme of antibody conjugated, Raman-tagged hollow gold-silver nanospheres for specific targeting and multimodal imaging. Reproduced with permission from the ACS article<sup>47</sup>.

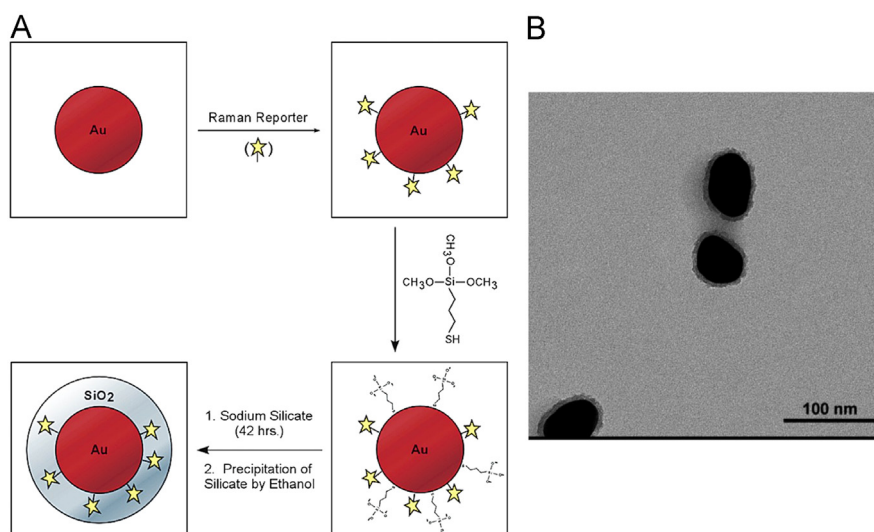


**Figure 3** (A) Schematic illustration of the synthesis of Au@SiO<sub>2</sub> with the Raman probe inside the nanoparticles. (B) TEM image of Au@SiO<sub>2</sub> nanoparticles. Reproduced with permission from the ACS article<sup>53</sup>.

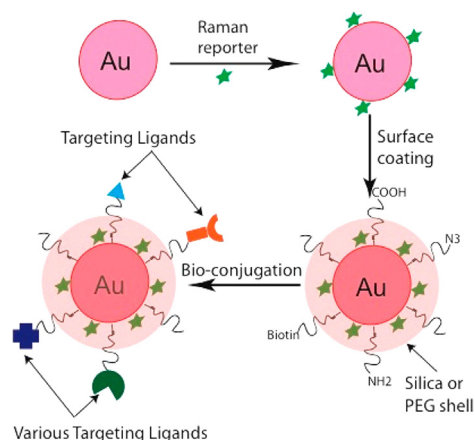


**Figure 4** Design and structure of nanoparticle tags, consisting of a metal nanoparticle core, adsorbed Raman probe molecules on the metal surface (green stars), a biocompatible layer (orange layer), and targeting ligands. Reproduced with permission from the ACS article<sup>32</sup>.

### 3. Tumor imaging-guided theranostics with SERS nanoparticles

The ability of nanoparticle-based platforms to gauge different targets simultaneously, sensitively and with multiplex imaging *in vivo*, is of considerable interest<sup>56–58</sup>. Zavaleta et al.<sup>59</sup> have reported that the functionality of multiplex imaging can be obtained *in vivo* after several Raman molecule probes were injected simultaneously with each molecule possessing an unparalleled spectrum (Fig. 5). The SERS nanoparticles arrive at the targeted site *in vivo* by one of two ways: they either accumulate in the body by enhanced permeability and retention effect (EPR)<sup>60</sup> or the receptor- or antibody-modified nanoparticles ensure the active targeting to particular tissues or tumors<sup>61–65</sup>. Previous *in vivo* studies depended on passive targeting to demonstrate that nanoparticles (>100 nm) are usually taken up by Kupffer cells of the reticuloendothelial system and subsequently accumulate in the

liver. Meanwhile, the signal of the nanoparticles in tumors will remain elevated while the concentration of administrated nanoparticles in blood returns to pre-injected levels. The passive targeting mode has been utilized in combination with the development of new instrumentation for SERS imaging *in vivo*.

To determine whether SERS signals can be obtained from PEGylated gold nanoparticles steeped *in vivo*, Qian et al.<sup>54</sup> have demonstrated that when small doses of SERS nanoparticles were administered to subcutaneous and deep muscular region in small animals, highly resolved SERS signals could be acquired from these regions. The *in vivo* SERS spectra measured are almost equal to those from *in vitro* saline samples. The sole distinction is that the absolute intensities are attenuated by 1–2 orders of magnitude when used *in vivo*. Because of the high signal to noise ratios of the SERS nanoparticles, the penetration depth can achieve about 1–2 cm, which is favorable for *in vivo* tumor detection or imaging.

ScFv antibody-modified gold nanoparticles were administered by intravenous injection to nude mice bearing a human head and neck tumor (Tu686) for *in vivo* tumor targeting ability studies (Fig. 6)<sup>54</sup>. The results showed that the obtained SERS spectra were noticeably different when the near-infrared (785 nm) laser beam was focused on the tumor region or other anatomical locations (e.g., the liver or a leg) 5 h after a SERS nanoparticle injection. More concretely, signal intensities between the targeted and nontargeted nanoparticles at the tumor site were distinguishable. Meanwhile, the SERS signals from the nonspecific liver are non-distinguishable. This study indicates that the ScFv-conjugated gold nanoparticles are effective for EGFR-positive tumor targeting performance *in vivo*. Time-dependent SERS results further demonstrate that the SERS nanoparticles accumulate in the tumor gradually 4–6 h after administration, and subsequently, the majority of the accumulated nanoparticles remained in the tumor site for more than 24 or 48 h.

One of the first examples of *in vivo* imaging of tumors was reported in 2012, which made use of a gold core/silica shell/Gd-coated nanoparticle that allowed triple modality imaging of brain tumors using SERS, MRI and photoacoustic imaging (Fig. 7)<sup>66</sup>. This nanoparticle construct did not use a targeting moiety on its surface,

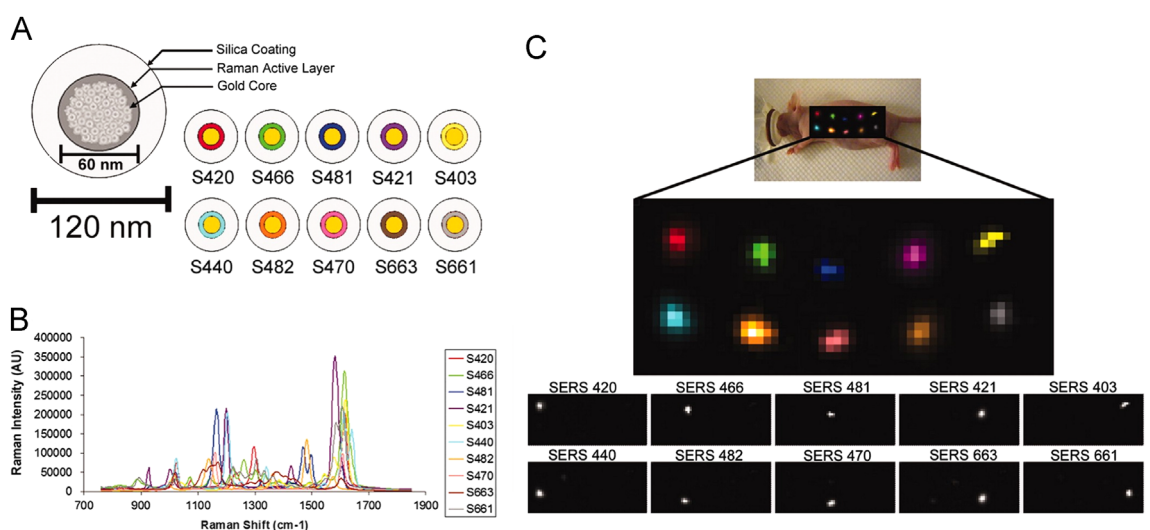


**Figure 5** (A) Schematic illustration of 10 SERS nanoparticles. The core is a gold nanoparticle and the Raman molecule adsorbed on the surface. Subsequently, a silica shell is coated on the surface as a protective layer. (B) The Raman spectra of 10 SERS nanoparticles depicted in (A). (C) The application of 10 different SERS nanoparticles *in vivo* to evaluate the multiplex imaging functionality. Reproduced with permission from the PNAS article<sup>59</sup>.

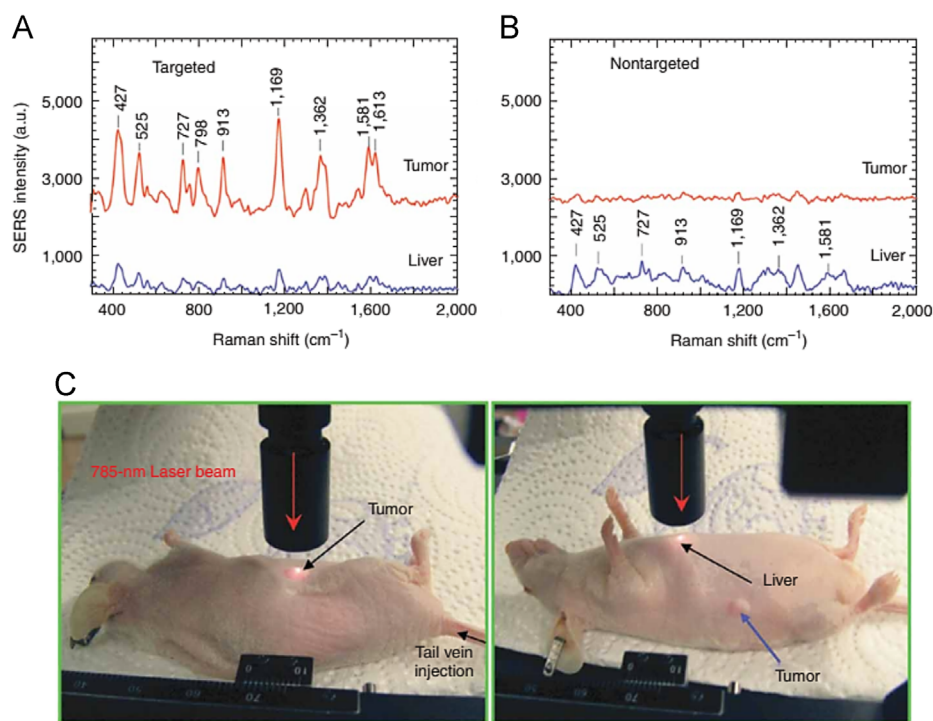


**Figure 6** (A and B) SERS spectra acquired from the tumor and liver site by using the active targeted (A) and nontargeted (B) SERS nanoparticles. Two nude mice with a human head-and-neck squamous cell carcinoma (Tu686) xenograft tumor (3-mm diameter) were systemically injected with the ScFv EGFR-modified SERS or PEGylated SERS nanoparticles. The SERS spectra were measured after administration for 5 h. (C) Photographs show a 785 nm laser beam focused on the tumor site or on the anatomical region of liver. *In vivo* SERS spectra were acquired from the tumor region (red line) and the liver region (blue line) after 785 nm laser excitation. The spectra had already subtracted the background. The Raman probe molecule is malachite green and the Laser excitation power is 20 mW. Reproduced with permission from The NPG article<sup>54</sup>.

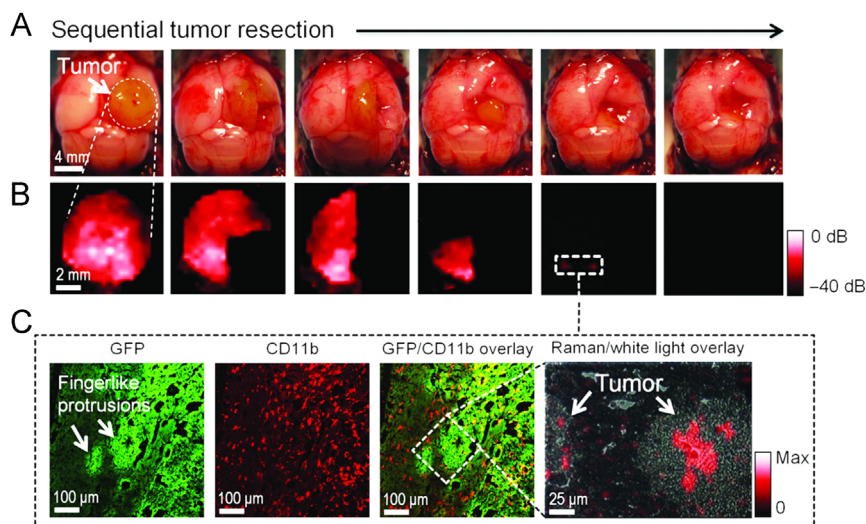


**Figure 7** Raman imaging-guided intraoperative surgery using a gold core/silica shell/Gd-coated nanoparticle. (A and B) The live tumor-bearing mice underwent craniotomy under general anesthesia. Quarters of the tumor site were sequentially resected and Raman imaging was taken after each resection step until the tumor site had been completely removed. After partial resection several minimal foci of Raman signal could be found in the removed section. The Raman color scale is shown in red (from -40 to 0 dB). (C) The histological analysis of these foci indicates that the infiltrative pattern of the tumor, which formed finger-like protrusions into the surrounding brain tissue. The Raman signal of these protrusions was acquired as shown in the Raman microscopy image, indicating that the SERS nanoparticles were a selective presence. The Raman signal is shown in a linear red color scale. Reproduced with permission from The NPG article<sup>66</sup>.

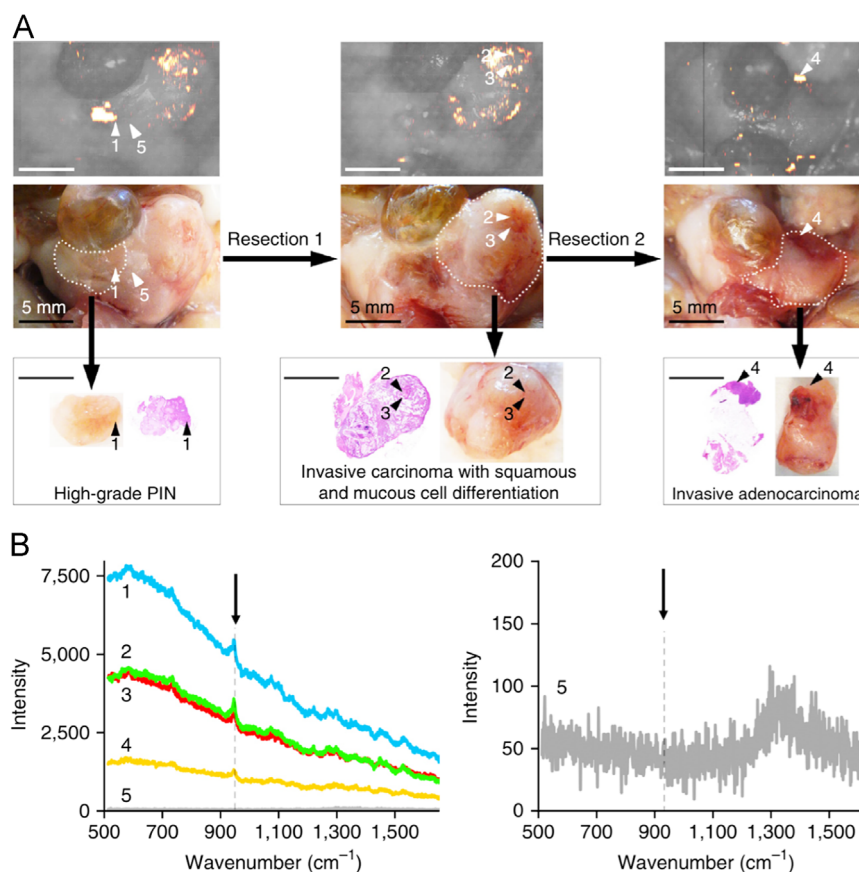


**Figure 8** SERS imaging of a prostate neoplasia. (A) SERS image-guided surgical resection procedure of *in-situ* prostate neoplasia of a Hi-Myc mouse which was injected intravenously with SERS nanoparticles. Raman images are on the top side and photos are of the central location. Raman image-guided surgical resection was performed on lesion 1 (along the dotted line in the left-hand image). Subsequently, Raman imaging was used for the second resection procedure (along the dotted line in the center image). Raman imaging was further taken after the procedure of resection 2 to screen for remaining tumor tissue. A residual lesion 4 was found and biopsied (dotted line in right-hand image). (Bottom) Histopathological examination of H&E-stained sections of the excised tissues 1-4 identified lesion 1 as high-grade prostate intraepithelial neoplasia and lesions 2-4 as advanced prostate cancer. (B) The left Raman spectra of lesions 1-4 and normal prostate tissue 5 adjacent to lesion 1. The arrow indicates the diagnostic  $950\text{ cm}^{-1}$  band of the injected SERS nanoparticles. The right intensity is scaled between 0 and 200 to show the Raman spectrum of normal prostate tissue. Scale bars are 5 mm. Reproduced with permission from the NPG article<sup>67</sup>.

relying on the EPR effect for passive accumulation within the glioblastoma tumor site. It allowed precise detection of the main tumor and microscopic extensions, and the feasibility of *in vivo* tumor resections based on the SERS signal was demonstrated for the first time. Importantly, it was also shown that no nanoparticles accumulated in the healthy brain, an observation establishing targeting specificity. However, when my group continued this work and tested the same nanoparticles in other extracranial tumor models, the resultant SERS signal was not found to be sufficient to allow robust cancer imaging. The Hi-Myc mouse was systemically administered with the SERS nanoparticles and subsequently, the *in-situ* Raman imaging of the prostate was carefully studied, which is shown in Fig. 8<sup>67</sup>. After lesion 1 was resected by the Raman-guided method, secondary Raman imaging was performed to remove the tumor section of lesions 2 and 3. During the Raman guided surgical resection procedure of lesions 2 and 3, it was found that these two sections contained invasive carcinoma of squamous and mucous cell differentiation. After the resection procedure 2, a Raman scan was taken as the final step. Residual SERS signal was discovered and lesion 4 was recognized, and biopsy results confirmed it to be invasive adenocarcinoma. As depicted in Fig. 8B, the characteristic

band around  $950\text{ cm}^{-1}$  of the SERS nanoparticles was evident in all identified premalignant and malignant prostate lesions, but not in normal prostate tissue.

Generally, the large surface-to-volume ratios of nanomaterials allow the combination of multiple diagnostic and therapeutic agents within one system. Integrating SERS nanoparticles with both diagnostic images (SERS imaging) and therapeutic functionality (photothermal, photodynamic and chemotherapy) is an ultimate goal, named a “theranostic” nanoplatform<sup>68,69</sup>.

Recently, SERS-guided theranostic nanoplatforms based on smart designs of SERS tags for tumor therapy have attracted considerable attention. Zhang et al.<sup>70</sup> functionalized the SERS gold nanorods with the photosensitizer dye protoporphyrin IX (PpIX) for photodynamic therapy (PDT). The PDT/SERS composites combine gold nanorods with DTTC Raman reporters encased by a silica shell which is later functionalized with PEG ligands and PpIX photosensitizers. This study indicated that SERS probes were found to facilitate the PDT ability of PpIX. Jung et al.<sup>71</sup> synthesized a theranostic agent consisting of a 10 nm gold nanosphere modified with pH-responsive ligands and Raman probes molecules attached to the surface (Fig. 9). This composite agent exhibited pH-triggered aggregation leading to

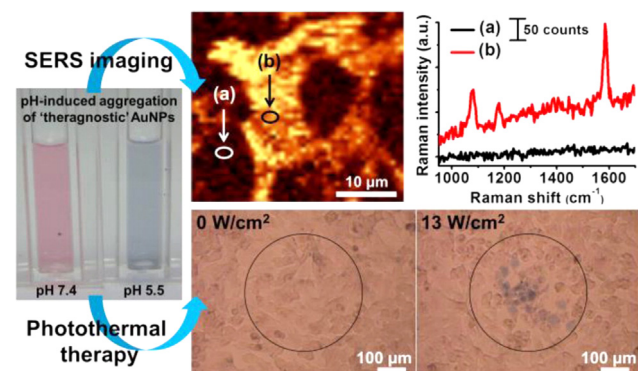


**Figure 9** Nanoparticle-based probe that can be used for a “turn-on” theranostic agent for simultaneous Raman imaging/diagnosis and photothermal therapy. Reproduced with permission from the ACS article<sup>71</sup>.

favorable Raman imaging performance and externally responsive photothermal efficacy when in a cancerous local environment. Jin et al.<sup>72</sup> developed a SERS theranostic platform consisted of metallic Au@Ag core-shell rodlike nanomaterials with embedded Raman reporters (Fig. 10). The localized surface plasmon resonance of these nanorods can be tuned from UV to NIR region, leading to highly tunable SERS and PT properties. Their study demonstrated that a thin Ag shell cover can be designed as multifunctional NIR theranostic probes that combine enhanced photothermal therapy capability.

Multifunctional metal-based nanoplatforms have been widely investigated for their potential in bioimaging, diagnostics, and photodynamic (PDT) therapy. Simon et al.<sup>73</sup> reported 3-dimensional (3-D) close-packed nanoassemblies of gold nanoparticles coated with Pluronic block copolymer (F127) polymer (Fig. 11). Methylene blue (MB) molecules, employed as both the optical label and photosensitizing drug, were loaded. The fabricated nanoassemblies offered optical imaging of murine colon carcinoma cells (C-26) *via* both Raman and fluorescence imaging collected from MB molecules. Furthermore, the photodynamic therapeutic performance of MB-loaded gold nanoaggregates against C-26 cancer cells was demonstrated.

Apart from the PTT- and PDT-functionalized SERS nanoparticles, the application of plasmonic-enhanced Raman imaging and chemotherapeutics delivery is gaining increasing attention (Fig. 12)<sup>74</sup>. A new theranostic nanoparticle for simultaneously evaluating drug-scattering, cellular imaging and Raman-scattering molecular vibration signals has been reported. This multifunctional nanoparticle provided real-time monitoring of the anticancer drug release process and *in vivo* biodistribution. The *in vivo* SERS detection of this system holds great promise for application in image-guided cancer chemotherapy.

This nanoplatform composed of therapeutic functionalities and SERS imaging provides exciting perspectives for imaging-guided synergistic therapy and beyond in a nanoparticle construct<sup>75–79</sup>. One could also overcome the limitations of mono-SERS performance. These smart “theranostic” SERS nanoplatforms will increase the opportunities for clinical applications.

#### 4. SERS nanoparticles for biosensing

Studies to identify tumor margins or to detect cancer *in vivo* have been discussed in this review article so far. However, the application of SERS toward the detection of tumor cells or biomarkers has not been described yet. Biomarker detection means

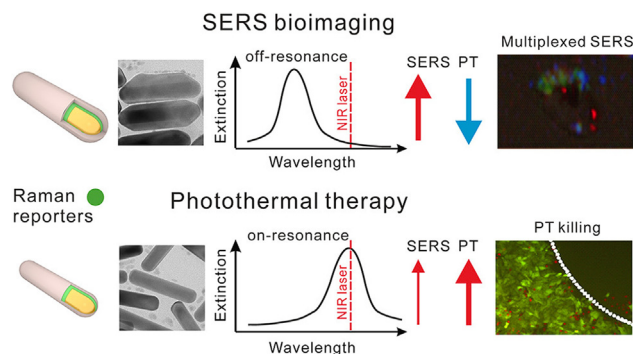


**Figure 10** Design strategy to fabricate SERS nanoparticles with embedded Raman reporters for bioimaging and photothermal therapy (PTT). On-resonant probes with a thin Ag shell show a moderate SERS performance and maximized photothermal (PT) effect, whereas off-resonant probes with a thick Ag shell show super high SERS performance and minimized PT effect. Reproduced with permission from the ACS article<sup>72</sup>.

identifying molecular indicators of disease in clinical samples, such as blood or urine. Many biomarkers associated with cancer can be identified in very low concentration. Detection methods have been widely developed, including enzyme-linked immunoassay (ELISA), radioactive immunoassays, Western blot, mass spectrometry (MS), or a combination thereof<sup>80–82</sup>. However, the SERS methods possess high sensitivity and can be multiplexed over many samples in addition to having a wide working range, offering the possibility of biomarker detection in whole blood with analyte concentrations spanning several orders of magnitude. Zhou et al.<sup>83</sup> have employed DNA-mediated SERS phenomenon of single-walled carbon nanotubes (SWNTs) to detect an extensive range of ctDNAs in human blood *in vitro*, ultrasensitively (Fig. 13). Combining the high-performance of the ctDNA recognition ability of the designed triple-helix molecular switch and RNase HII enzyme-assisted amplification, the DNA-mediated SERS enhancement of SWNTs could achieve detection sensitivity as low as 0.3 fmol/L, which provides the potential feasibility of point-of-care testing in clinical diagnosis.

At present, many patients suffer from diabetes mellitus due to insulin dysfunction. It is well known that insulin regulates glucose metabolism. The commonly used method is to take a small sample of the patient’s blood. However, this detection approach is painful. Therefore, the future aim is to make progress toward *in vivo* detection, with minimally damaging sensing. The Van Duyne group<sup>84</sup> modified a silver film over a nanosphere surface with alkanethiol molecules to form a partition layer to quantitatively detect glucose by SERS. However, this approach needs further characterization, including the optimum number or concentration of alkanethiol molecules, the wavelength and power of the laser, and the appropriate acquisition time.

#### 5. Conclusions and outlook

SERS nanoparticles have been used as a new form of molecular imaging agents<sup>85</sup> to diagnose cancer or intratumoral heterogeneity, and during the past few years has shown promise in clinical translation. However, current Raman scanners lack the wide field of view and rapid image acquisition speeds, which severely hinders the clinical application of SERS nanoparticles.

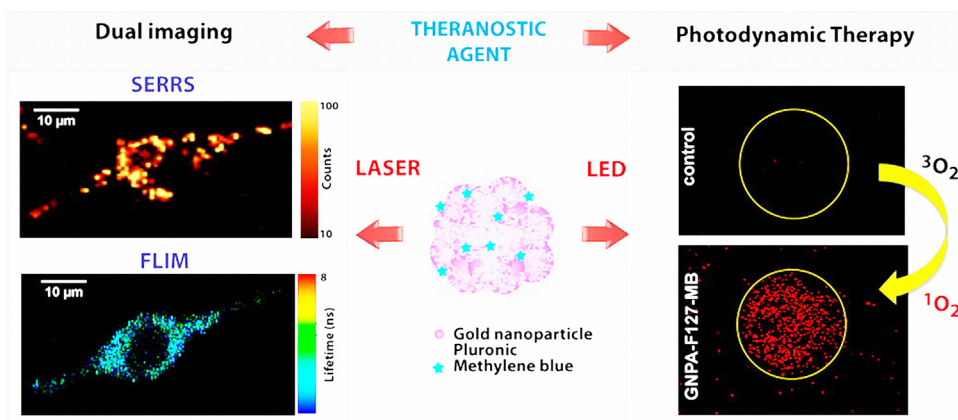


**Figure 11** Scheme for the synthesis of gold nanoparticles and polymer stabilization for bioimaging and photodynamic therapy (PDT). Reproduced with permission from the ACS article<sup>73</sup>.

Nevertheless, efforts are being made to overcome these obstacles. Developing deep tumor detection (or imaging) performance is another aspect of application in oncology for SERS nanoparticles. A Raman endoscope that fits into the instrument channel of a conventional white light endoscope already exists. Therefore, developing deep tissue Raman detectors is highly promising.

The above-mentioned discussion focuses on technical problems. Currently, the real bottleneck in the clinical application of SERS nanoparticles is not just the detection technology, but regulatory approval of the nanoparticles themselves, with concerns about biotoxicity *in vivo*. The particle's safety, pharmacokinetics,

clearance properties, and radiation dosimetry will be a chief issue for use *in vivo*. Toward this end, SERS nanoparticles made of Food and Drug Administration (FDA)-approved materials such as gold and silica have shown good biocompatibility in extensive animal studies, and other types of gold and gold-silica nanoparticles for cancer therapy have already advanced into clinical trials.

The increased precision in visualizing the true extent of tumor margins provided by the SERS signal could advance the accuracy with which cancer can be diagnosed or destroyed, thus providing great promise. Increased accuracy means that less tumor tissue is left behind, and more healthy tissue can be spared. This could

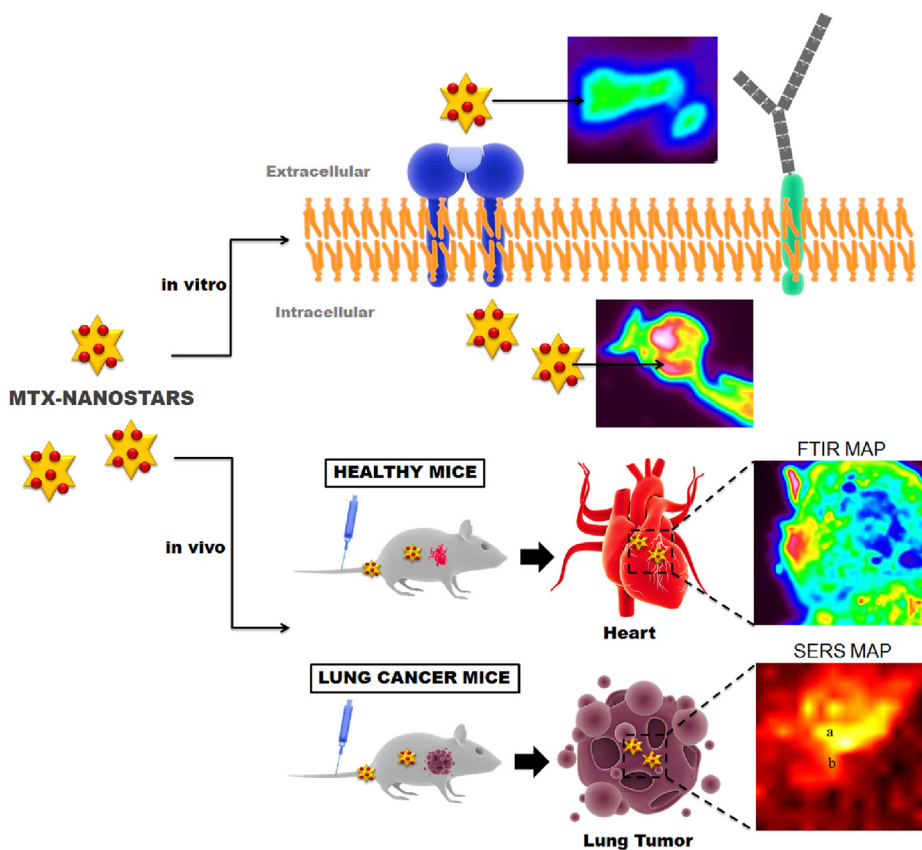


**Figure 12** Gold Nanostars for theranostics: intracellular and *in vivo* SERS detection combined with real-time drug delivery using plasmonic-tunable Raman/FTIR imaging. Reproduced with permission from the Elsevier article<sup>74</sup>.

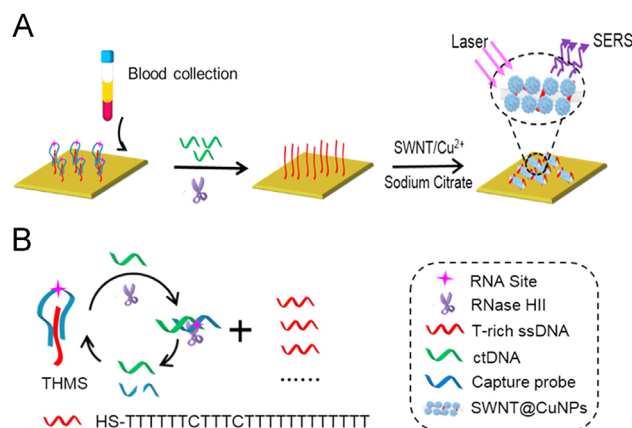


**Figure 13** (A) Construction of SWNT-based SERS assay coupling with RNase HIII-assisted amplification for highly sensitive detection of ctDNA in human blood. The enlarged image illustrates T-rich DNA-mediated growth of CuNPs to enhance the SERS signal of SWNTs. (B) Mechanism of RNase HIII-assisted THMS-based amplified recognition to produce numerous T-rich ssDNAs. Reproduced with permission from ACS article<sup>83</sup>.

improve patient outcomes not only during classical open surgeries but also especially in the emerging fields of minimally invasive and robotically assisted procedures.

In brief, SERS nanoparticles possess favorable advantages over traditional imaging models, offering much higher sensitivity, nearly perfect signal specificity, and unparalleled multiplexing capabilities. There are driving forces to exploit these features for image-guided tumor therapy and detection. The next breakthrough is likely to be the development of SERS nanoparticles and spectroscopic devices for clinical applications. Moreover, though there still are some difficulties to be solved, SERS nanoparticles will have significant opportunities for clinical translation in the future.

## Acknowledgments

This work was supported by the National Key Research and Development Program of China (2016YFA0100900), the National Natural Science Foundation of China (No. 81671748), China Postdoctoral Science Foundation (2017M620243), and the Project of Chinese Thousand Youth Talents.

## References

- Nie S, Emory SR. Probing single molecules and single nanoparticles by surface-enhanced Raman scattering. *Science* 1997;**275**:1102–6.
- Reguera J, Langer J, Jiménez de Aberasturi D, Liz-Marzan LM. Anisotropic metal nanoparticles for surface enhanced Raman scattering. *Chem Soc Rev* 2017;**46**:3866–85.
- Lyon LA, Keating CD, Fox AP, Baker BE, He L, Nicewarner SR, et al. Raman spectroscopy. *Anal Chem* 1998;**70**:341–62.
- Raman CV, Krishnan KS. A new type of secondary radiation. *Nature* 1928;**121**:501–2.
- Campion A, Kambhampati P. Surface-enhanced Raman scattering. *Chem Soc Rev* 1998;**27**:241–50.
- Fleischmann M, Hendra PJ, McQuillan AJ. Raman spectra of pyridine adsorbed at a silver electrode. *Chem Phys Lett* 1974;**26**:163–6.
- Jeanmaire DL, Van Duyne RP. Surface Raman spectroelectrochemistry: part I. Heterocyclic, aromatic, and aliphatic amines adsorbed on the anodized silver electrode. *J Electroanal Chem Interface* 1977;**84**:1–20.
- Albrecht MG, Creighton JA. Anomalously intense Raman spectra of pyridine at a silver electrode. *J Am Chem Soc* 1977;**99**:5215–7.
- Kneipp K, Wang Y, Kneipp H, Perelman LT, Itzkan I, Dasari RR, et al. Single molecule detection using surface-enhanced Raman scattering. *Phys Rev Lett* 1997;**78**:1667–70.
- Xu H, Bjerneld EJ, Kall M, Borjesson L. Spectroscopy of single hemoglobin molecules by surface enhanced Raman scattering. *Phys Rev Lett* 1999;**83**:4357–60.
- Le Ru EC, Etchegoin PG, Meyer M. Enhancement factor distribution around a single surface-enhanced Raman scattering hot spot and its relation to single molecule detection. *J Chem Phys* 2006;**125**:204701.
- Sonntag MD, Klingsporn JM, Zrimsek AB, Sharma B, Ruvuna LK, Van Duyne RP. Molecular plasmonics for nanoscale spectroscopy. *Chem Soc Rev* 2014;**43**:1230–47.
- Orendorff CJ, Gole A, Sau TK, Murphy CJ. Surface-enhanced Raman spectroscopy of self-assembled monolayers: sandwich architecture and nanoparticle shape dependence. *Anal Chem* 2005;**77**:3261–6.
- Huefner A, Kuan WL, Müller KH, Skepper JN, Barker RA, Mahajan S. Characterization and visualization of vesicles in the endo-lysosomal pathway with surface-enhanced Raman spectroscopy and chemometrics. *ACS Nano* 2016;**10**:307–16.
- Cialla-May D, Zheng XS, Weber K, Popp J. Recent progress in surface-enhanced Raman spectroscopy for biological and biomedical applications: from cells to clinics. *Chem Soc Rev* 2017;**46**:3945–61.
- Lussier F, Brulé T, Vishwakarma M, Das T, Spatz JP, Masson JF. Dynamic-SERS optophysiology: a nanosensor for monitoring cell secretion events. *Nano Lett* 2016;**16**:3866–71.
- Wang DS, Kerker M. Enhanced Raman scattering by molecules adsorbed at the surface of colloidal spheroids. *Phys Rev B* 1981;**24**:1777–90.
- Novotny L, Hecht B, Pohl DW. Interference of locally excited surface plasmons. *J Appl Phys* 1997;**81**:1798–806.
- Stöckle RM, Suh YD, Deckert V, Zenobi R. Nanoscale chemical analysis by tip-enhanced Raman spectroscopy. *Chem Phys Lett* 2000;**318**:131–6.
- Hayazawa N, Inouye Y, Sekkat Z, Kawata S. Metallized tip amplification of near-field Raman scattering. *Opt Commun* 2000;**183**:333–6.
- Anderson MS. Locally enhanced Raman spectroscopy with an atomic force microscope. *Appl Phys Lett* 2000;**76**:3130–2.
- Brown LO, Doorn SK. Optimization of the preparation of glass-coated, dye-tagged metal nanoparticles as SERS substrates. *Langmuir* 2008;**24**:2178–85.

23. Krug JT, Wang GD, Emory SR, Nie S. Efficient Raman enhancement and intermittent light emission observed in single gold nanocrystals. *J Am Chem Soc* 1999;**121**:9208–14.
24. Sun X, Li Y. Colloidal carbon spheres and their core/shell structures with noble-metal nanoparticles. *Angew Chem Int Ed Engl* 2004;**43**:597–601.
25. Mahmoud MA, El-Sayed MA. Different plasmon sensing behavior of silver and gold nanorods. *J Phys Chem Lett* 2013;**4**:1541–5.
26. Orendorff CJ, Gearheart L, Jana NR, Murphy CJ. Aspect ratio dependence on surface enhanced Raman scattering using silver and gold nanorod substrates. *Phys Chem Chem Phys* 2006;**8**:165–70.
27. Yang Y, Zhong XL, Zhang Q, Blackstad LG, Fu ZW, Li ZY, et al. The role of etching in the formation of Ag nanoplates with straight, curved and wavy edges and comparison of their SERS properties. *Small* 2014;**10**:1430–7.
28. Skrabalak SE, Au L, Li X, Xia Y. Facile synthesis of Ag nanocubes and Au nanocages. *Nat Protoc* 2007;**2**:2182–90.
29. Lee SJ, Morrill AR, Moskovits M. Hot spots in silver nanowire bundles for surface-enhanced Raman spectroscopy. *J Am Chem Soc* 2006;**128**:2200–1.
30. Etchegoin PG, Galloway C, Le Ru E. Polarization-dependent effects in surface-enhanced Raman scattering (SERS). *Phys Chem Chem Phys* 2006;**8**:2624–8.
31. Yuan H, Khoury CG, Hwang H, Wilson CM, Grant GA, Vo-Dinh T. Gold nanostars: surfactant-free synthesis, 3D modelling, and two-photon photoluminescence imaging. *Nanotechnology* 2012;**23**:075102.
32. Lane LA, Qian X, Nie S. SERS Nanoparticles in medicine: from label-free detection to spectroscopic tagging. *Chem Rev* 2015;**115**:10489–529.
33. Li JF, Zhang YJ, Ding SY, Panneerselvam R, Tian ZQ. Core-shell nanoparticle-enhanced Raman spectroscopy. *Chem Rev* 2017;**117**:5002–69.
34. Huang J, Guo M, Ke H, Zong C, Ren B, Liu G, et al. Rational design and synthesis of  $\gamma\text{Fe}_2\text{O}_3/\text{Au}$  magnetic gold nanoflowers for efficient cancer theranostics. *Adv Mater* 2015;**27**:5049–56.
35. Gao X, Yue Q, Liu Z, Ke M, Zhou X, Li S, et al. Guiding brain-tumor surgery via blood-brain-barrier-permeable gold nanoprobe with acid-triggered MRI/SERS signals. *Adv Mater* 2017;**29**:1603917.
36. Iacono P, Karabeber H, Kircher MF. A “schizophonic” all-In-one nanoparticle coating for multiplexed SE(R)RS biomedical imaging. *Angew Chem Int Ed Engl* 2014;**53**:11756–61.
37. Xie J, Zhang Q, Lee JY, Wang DI. The synthesis of SERS-active gold nanoflower tags for *in vivo* applications. *ACS Nano* 2008;**2**:2473–80.
38. Andreou C, Neuschmelting V, Tschaharganeh DF, Huang CH, Oseledchik A, Iacono P, et al. Imaging of liver tumors using surface-enhanced Raman scattering nanoparticles. *ACS Nano* 2016;**10**:5015–26.
39. Vendrell M, Maiti KK, Dhaliwal K, Chang YT. Surface-enhanced Raman scattering in cancer detection and imaging. *Trends Biotechnol* 2013;**31**:249–57.
40. Tao A, Kim F, Hess C, Goldberger J, He R, Sun Y, et al. Langmuir-blodgett silver nanowire monolayers for molecular sensing using surface-enhanced Raman spectroscopy. *Nano Lett* 2003;**3**:1229–33.
41. Talley CE, Jackson JB, Oubre C, Grady NK, Hollars CW, Lane SM, et al. Surface-enhanced Raman scattering from individual Au nanoparticles and nanoparticle dimer substrates. *Nano Lett* 2005;**5**:1569–74.
42. Chen LY, Yu JS, Fujita T, Chen MW. Nanoporous copper with tunable nanoporosity for SERS applications. *Adv Funct Mater* 2009;**19**:1221–6.
43. Camden JP, Dieringer JA, Wang Y, Masiello DJ, Marks LD, Schatz GC, et al. Probing the structure of single-molecule surface-enhanced Raman scattering hot spots. *J Am Chem Soc* 2008;**130**:12616–7.
44. Park JH, Von Maltzahn G, Ong LL, Centrone A, Hatton TA, Ruoslahti E, et al. Cooperative nanoparticles for tumor detection and photo-thermally triggered drug delivery. *Adv Mater* 2010;**22**:880–5.
45. Henry AI, Sharma B, Cardinal MF, Kurouski D, Van Duyne RP. Surface-enhanced Raman spectroscopy biosensing: *in vivo* diagnostics and multimodal imaging. *Anal Chem* 2016;**88**:6638–47.
46. Potara M, Nagy-Simon T, Craciun AM, Suarasan S, Licarete E, Imre-Lucaci F, et al. Carboplatin-loaded, Raman-encoded, chitosan-coated silver nanotriangles as multimodal traceable nanotherapeutic delivery systems and pH reporters inside human ovarian cancer cells. *ACS Appl Mater Interfaces* 2017;**9**:32565–76.
47. Nagy-Simon T, Tatar AS, Craciun AM, Vulpoi A, Jurj MA, Florea A, et al. Antibody conjugated, Raman tagged hollow gold-silver nanospheres for specific targeting and multimodal dark-field/SERS/two-photon-FLIM imaging of CD19(+) B lymphoblasts. *ACS Appl Mater Interfaces* 2017;**9**:21155–68.
48. Wang C, Chen Y, Wang T, Ma ZF, Su ZM. Monodispersed gold nanorod-embedded silica particles as novel Raman labels for biosensing. *Adv Funct Mater* 2008;**18**:355–61.
49. Campbell JL, Sorelle ED, Ilovich O, Liba O, James ML, Qiu Z, et al. Multimodal assessment of SERS nanoparticle biodistribution post ingestion reveals new potential for clinical translation of Raman imaging. *Biomaterials* 2017;**135**:42–52.
50. Andreou C, Kishore SA, Kircher MF. Surface-enhanced Raman spectroscopy: a new modality for cancer imaging. *J Nucl Med* 2015;**56**:1295–9.
51. Keren S, Zavaleta C, Cheng Z, Da La Zerd A, Gheysens O, Gambhir SS. Noninvasive molecular imaging of small living subjects using Raman spectroscopy. *Proc Natl Acad Sci U S A* 2008;**105**:5844–9.
52. Li JF, Anema JR, Wandlowski T, Tian ZQ. Dielectric shell isolated and graphene shell isolated nanoparticle enhanced Raman spectroscopies and their applications. *Chem Soc Rev* 2015;**44**:8399–409.
53. Doering WE, Nie S. Spectroscopic tags using dye-embedded nanoparticles and surface-enhanced Raman scattering. *Anal Chem* 2003;**75**:6171–6.
54. Qian X, Peng XH, Ansari DO, Yin-Goen Q, Chen GZ, Shin DM, et al. *In vivo* tumor targeting and spectroscopic detection with surface-enhanced Raman nanoparticle tags. *Nat Biotechnol* 2008;**26**:83–90.
55. Cao YC, Jin R, Mirkin CA. Nanoparticles with Raman spectroscopic fingerprints for DNA and RNA detection. *Science* 2002;**297**:1536–40.
56. Gao HL. Progress and perspectives on targeting nanoparticles for brain drug delivery. *Acta Pharm Sin B* 2016;**6**:268–86.
57. Huang R, Harmsen S, Samii JM, Karabeber H, Pitter KL, Holland EC, et al. High precision imaging of microscopic spread of glioblastoma with a targeted ultrasensitive SERS molecular imaging probe. *Theranostics* 2016;**6**:1075–84.
58. Mallia RJ, McVeigh PZ, Fisher CJ, Veilleux I, Wilson BC. Wide-field multiplexed imaging of EGFR-targeted cancers using topical application of NIR SERS nanoprobe. *Nanomedicine* 2015;**10**:89–101.
59. Zavaleta CL, Smith BR, Walton I, Doering W, Davis G, Shojaei B, et al. Multiplexed imaging of surface enhanced Raman scattering nanotags in living mice using noninvasive Raman spectroscopy. *Proc Natl Acad Sci U S A* 2009;**106**:13511–6.
60. Maeda H, Wu J, Sawa T, Matsumura Y, Hori K. Tumor vascular permeability and the EPR effect in macromolecular therapeutics: a review. *J Control Release* 2000;**65**:271–84.
61. Oseledchik A, Andreou C, Wall MA, Kircher MF. Folate-targeted surface-enhanced resonance Raman scattering nanoprobe ratiometry for detection of microscopic ovarian cancer. *ACS Nano* 2017;**11**:1488–97.
62. Jina K, Luo ZM, Zhang B, Pang Z. Biomimetic nanoparticles for inflammation targeting. *Acta Pharm Sin B* 2018;**8**:23–33.
63. Lia RX, He YW, Zhang SY, Qin J, Wang J. Cell membrane-based nanoparticles: a new biomimetic platform for tumor diagnosis and treatment. *Acta Pharm Sin B* 2018;**8**:14–22.
64. Chen X, Liu L, Jiang C. Charge-reversal nanoparticles: novel targeted drug delivery carriers. *Acta Pharm Sin B* 2016;**6**:261–7.
65. Ruan CH, Liu LH, Lu YF, Zhang Y, He X, Chen XL, et al. Substance P-modified human serum albumin nanoparticles loaded with paclitaxel for targeted therapy of glioma. *Acta Pharm Sin B* 2018;**8**:85–96.
66. Kircher MF, De La Zerd A, Jokerst JV, Zavaleta CL, Kempen PJ, Mitra E, et al. A brain tumor molecular imaging strategy using a new triple-modality MRI-photoacoustic-Raman nanoparticle. *Nat Med* 2012;**18**:829–34.

67. Harmsen S, Wall MA, Huang R, Kircher MF. Cancer imaging using surface-enhanced resonance Raman scattering nanoparticles. *Nat Protoc* 2017;**12**:1400–14.
68. Popovtzer R, Agrawal A, Kotov NA, Popovtzer A, Balter J, Carey TE, et al. Targeted gold nanoparticles enable molecular CT imaging of cancer. *Nano Lett* 2008;**8**:4593–6.
69. Harmsen S, Bedics MA, Wall MA, Huang R, Detty MR, Kircher MF. Rational design of a chalcogenopyrylium-based surface-enhanced resonance Raman scattering nanoprobe with attomolar sensitivity. *Nat Commun* 2015;**6**:6570.
70. Zhang Y, Qian J, Wang D, Wang Y, He S. Multifunctional gold nanorods with ultrahigh stability and tunability for *in vivo* fluorescence imaging, SERS detection, and photodynamic therapy. *Angew Chem Int Ed Engl* 2013;**52**:1148–51.
71. Jung S, Nam J, Hwang S, Park J, Hur J, Im K, et al. Theragnostic pH-sensitive gold nanoparticles for the selective surface enhanced raman scattering and photothermal cancer therapy. *Anal Chem* 2013;**85**:7674–81.
72. Jin X, Khlebtsov BN, Khanadeev VA, Khlebtsov NG, Ye J. Rational design of ultrabright SERS probes with embedded reporters for bioimaging and photothermal therapy. *ACS Appl Mater Interfaces* 2017;**9**:30387–97.
73. Simon T, Potara M, Gabudean AM, Licarete E, Banciu M, Astilean S. Designing theranostic agents based on pluronic stabilized gold nanoaggregates loaded with methylene blue for multimodal cell imaging and enhanced photodynamic therapy. *ACS Appl Mater Interfaces* 2015;**7**:16191–201.
74. Tian F, Conde J, Bao C, Chen YS, Curtin J, Cui D. Gold nanostars for efficient *in vitro* and *in vivo* real-time SERS detection and drug delivery via plasmonic-tunable Raman/FTIR imaging. *Biomaterials* 2016;**106**:87–97.
75. Oo Khaing MK, Yang Y, Hu Y, Gomez M, Du H, Wang H. Gold nanoparticle-enhanced and size-dependent generation of reactive oxygen species from protoporphyrin IX. *ACS Nano* 2012;**6**:1939–47.
76. Lu W, Singh AK, Khan SA, Senapati D, Yu H, Ray PC. Gold nanopopcorn-based targeted diagnosis, nanotherapy treatment, and *in situ* monitoring of photothermal therapy response of prostate cancer cells using surface-enhanced raman spectroscopy. *J Am Chem Soc* 2010;**132**:18103–14.
77. Tian L, Gandra N, Singamaneni S. Monitoring controlled release of payload from gold nanocages using surface enhanced raman scattering. *ACS Nano* 2013;**7**:4252–60.
78. Kim C, Cho EC, Chen J, Song KH, Au L, Favazza C, et al. *In vivo* molecular photoacoustic tomography of melanomas targeted by bioconjugated gold nanocages. *ACS Nano* 2010;**4**:4559–64.
79. Gao Y, Li Y, Chen J, Zhu SJ, Liu XH, Zhou LP, et al. Multifunctional gold nanostar-based nanocomposite: synthesis and application for noninvasive MR-SERS imaging-guided photothermal ablation. *Biomaterials* 2015;**60**:31–41.
80. Ambrosi A, Airo F, Merkoci A. Enhanced gold nanoparticle based ELISA for a breast cancer biomarker. *Anal Chem* 2010;**82**:1151–6.
81. Fortin T, Salvador A, Charrier JP, Lenz C, Lacoux X, Morla A, et al. Clinical quantitation of prostate-specific antigen biomarker in the low nanogram/milliliter range by conventional bore liquid chromatography–tandem mass spectrometry (multiple reaction monitoring) coupling and correlation with Elisa Tests. *Mol Cell Proteom* 2009;**8**:1006–15.
82. Bast RC, Klug TL, John E, Jenison E, Niloff JM, Lazarus H, et al. A radioimmunoassay using a monoclonal antibody to monitor the course of epithelial ovarian cancer. *N Engl J Med* 1983;**309**:883–7.
83. Zhou Q, Zheng J, Qing Z, Zheng M, Yang J, Yang S, et al. Detection of circulating tumor DNA in human blood via DNA-mediated surface-enhanced raman spectroscopy of single-walled carbon nanotubes. *Anal Chem* 2016;**88**:4759–65.
84. Shafer-Peltier KE, Haynes CL, Glucksberg MR, Van Duyne RP. Toward a glucose biosensor based on surface-enhanced Raman scattering. *J Am Chem Soc* 2003;**125**:588–93.
85. M.W. Li, Y.Y. Qiu, C.C. Fan, K. Cui, Y.M. Zhang and Z.Y. Xiao, Design of SERS nanoprobe for Raman imaging: materials, affecting factors and architectures, *Acta Pharm Sin B* 2018. Available from: <<http://dx.doi.org/10.1016/j.apsb.2018.01.010>> .